

3D-printed microfluidic-microwave device for droplet networks formation and characterisation

Kai Silver¹, Jin Li¹, *, Adrian Porch¹, William David Jamieson², Oliver Castell², Pantelitsa Dimitriou¹, Colin Kallnik¹, and David Barrow¹

¹School of Engineering, Cardiff University, The Parade, Cardiff, CF24 3AA, United Kingdom

²School of Pharmacy and Pharmaceutical Science, Cardiff University, King Edward VII Ave, Cardiff, CF10 3NB, United Kingdom

Corresponding author: Jin Li (E-mail: LiJ40@cardiff.ac.uk)

Supplementary Information

Table of Contents

Fig S1. Experimental setup

Fig S2. Experimental setup for microwave dielectric characterization of 3D-printed plastic samples.

Fig S3. Performance of MMDs with different 3D-printed dielectric substrate materials in the microwave characterisation of liquid samples.

Fig S4. Evaluation of the impact of eutectic filling conditions on MMD performance.

Fig S5. Aqueous droplets were collected from the outlet fluidic tubing into 3D-printed PLA square dishes.

Fig S6. Microwave readout distinguishing small and large droplets, facilitating droplet counting.

Fig S7. Examples of DIB networks with droplets encapsulating different dyes, formed by programmed fluidic inputs.

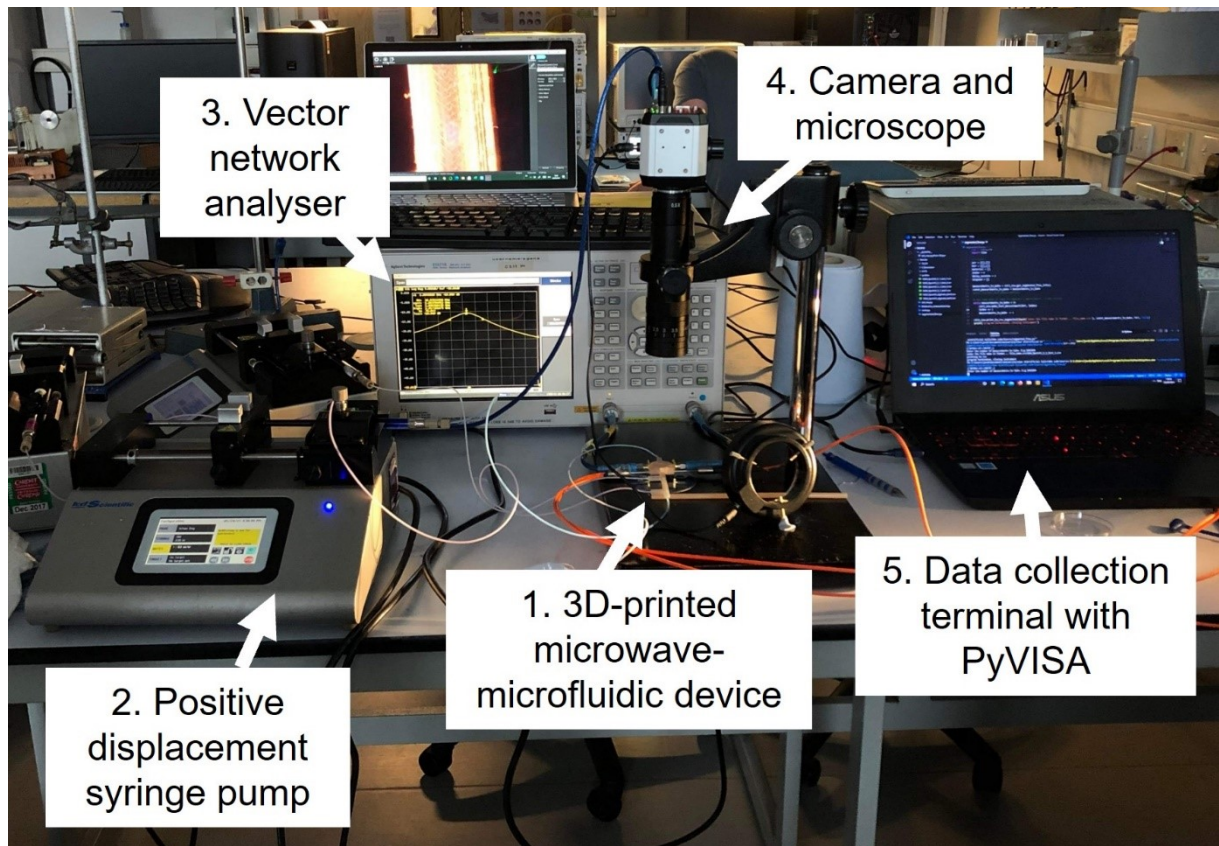
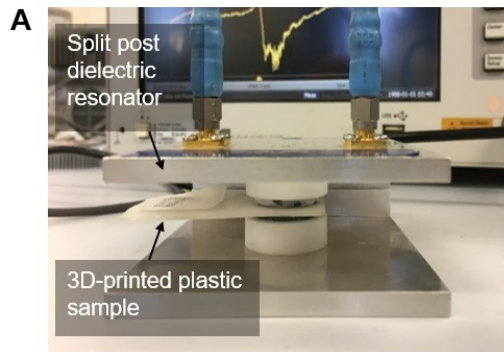


Fig S1. Experimental setup. The microwave-microfluidic device was connected to syringe pumps and a vector network analyser for fluid injection and microwave readout, respectively. A CCD camera, attached to an optical microscope, captured the flow of droplets within the microwave-microfluidic device. Microwave readouts were collected using customised code in PyVISA on a Windows-based laptop.



B

| Plastic sample (substrate material) | Printing infill (100%) | $\epsilon_1 \pm 3\%$ | $\epsilon_2 \pm 3\%$ |
|-------------------------------------|------------------------|----------------------|----------------------|
| COC | 100% | 5.35 | 0.010 |
| COC | 50% | 3.63 | 0.002 |
| PLA | 100% | 6.31 | 0.070 |
| Light weight PLA | 100% | 3.95 | 0.042 |
| Nylon | 100% | 7.44 | 0.350 |
| Polypropylene | 100% | 10.3 | 0.008 |

Fig S2. Experimental setup for microwave dielectric characterization of 3D-printed plastic samples. A. The setup utilised the cavity perturbation technique and used a VNA to measure the voltage transmission coefficient S_{21} . A bespoke split-post dielectric resonator operating at 2.7GHz was employed to assess the complex permittivity of the samples. **B.** Table showing the calculated complex permittivity values of various 3D-printed samples.

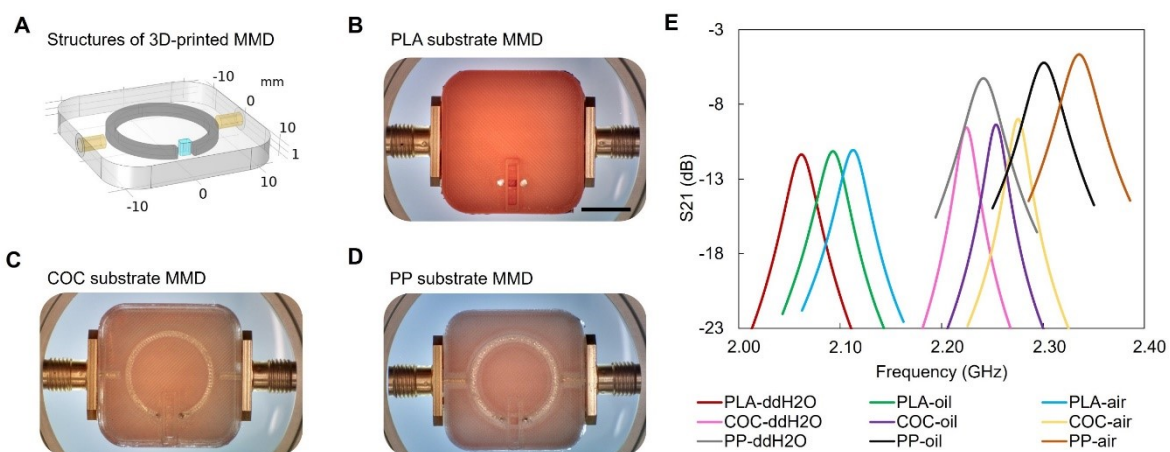
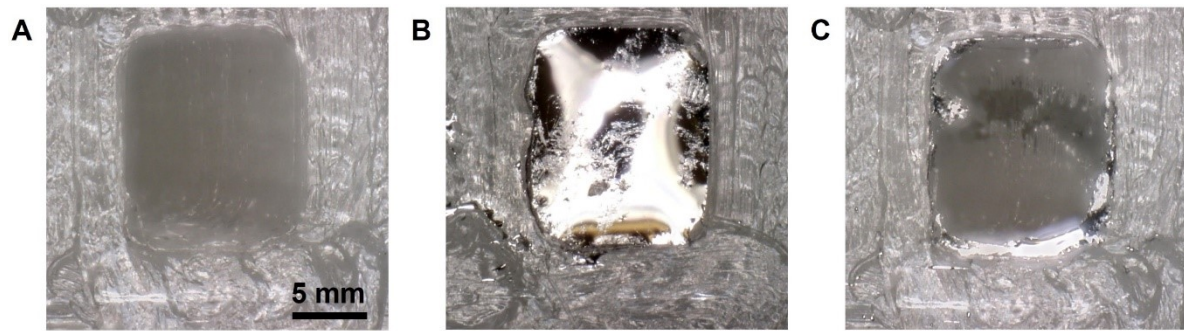


Fig S3. Performance of MMDs with different 3D-printed dielectric substrate materials in the microwave characterisation of liquid samples. **A** Structures of 3D-printed MMD with an open microfluidic chamber at the split-ring gap region. **B**. Samples of MMDs made from PLA, **C**. from COC and **D**. from PP (bottom) filaments. All MMDs were built from the identical geometrical design and printing settings, with a layer thickness of 0.1 mm and line width of 0.23 mm. Among these, the COC MMD exhibits superior microwave features, while PLA and PP were chosen for their chemical and physical properties suitable to various microfluidic applications. Scale bar denotes 1 cm. **E**. Microwave signatures (based on the magnitude of S_{21} measured by the VNA) obtained from using different MMDs to characterize various fluid materials within the gap region of the split-ring resonator.



D

| | Bandwidth (MHz) | Centre frequency (GHz) | Quality factor | Transmission loss (dB) |
|-----------------------------------|-----------------|------------------------|----------------|------------------------|
| Eutectic filled | 21.86 | 2.22 | 101.60 | -9.09 |
| Eutectic removed; thin layer left | 45.05 | 2.17 | 48.07 | -18.41 |

Fig S4. Evaluation of the impact of eutectic filling conditions on MMD performance. A-C. Sequential cross-sectional views of the ring resonator showing (a) the void channel, (b) channel filled with eutectic materials, and (c) after eutectic removal, with a thin layer of eutectic remaining on the ring channel wall. **D.** Table of microwave parameters for the split-ring microwave resonator before and after eutectic removal. The residual thin layer of eutectic facilitates microwave current transmission, confined to the skin depth, estimated at approximately $6 \mu\text{m}$ at 2.2 GHz. The microwave resonance is maintained, albeit with a slightly higher resonant frequency and lower Q-factor.

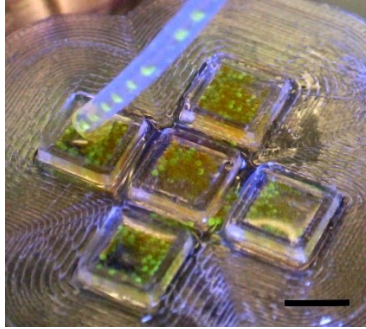


Fig S5. Aqueous droplets were collected from the outlet fluidic tubing into 3D-printed PLA square dishes . Scale bar denotes 1cm.

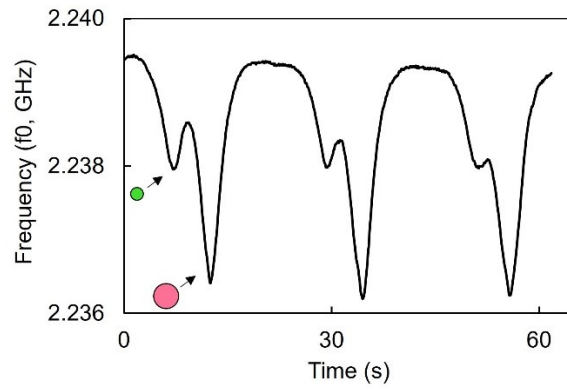


Fig S6. Microwave readout distinguishing small and large droplets, facilitating droplet counting. The W-shaped signatures are due to that the droplets were close to each other when flowing through the gap region of the split ring microwave resonator.

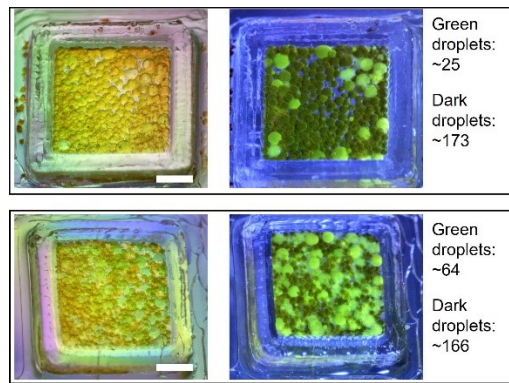


Fig S7. Examples of DIB networks with droplets encapsulating different dyes, formed by programmed fluidic inputs. Approximate droplet counts were derived from the microwave readouts.